

## ENERGY STREAMLINES IN THE VICINITY OF DISLOCATIONS OF A THREE-DIMENSIONAL WAVE FIELD

V.V. Kolosov

*Institute of Atmospheric Optics,  
Siberian Branch of the Russian Academy of Sciences, Tomsk  
Received August 7, 1996*

*Based on the analysis of general integral solution of wave equation (the Kirchhoff integral) in Fresnel approximation, a behavior of the energy streamlines is considered at improper points of three-dimensional optical field, i.e. phase front dislocations and saddles, where the amplitude and the transverse gradient of a field phase vanish. The peculiarities are revealed in the energy streamlines behavior that allow one to distinguish between two- and three dimensional wave field. The diffraction rays method is shown to be useful in constructing the spatial spiral streamlines based on known intensity distribution.*

*The interference patterns arising from the interference between speckle field and plane waves of various directions are analyzed. It is shown, that the interference pattern can take form of «fractured» twisting spiral. The fracture points therewith coincide with the speckle field dislocations. In the case of interference with various plane waves, the pattern essentially changes. Nevertheless, at the dislocation points, the direction of a tangent to the interference line holds constant for all patterns.*

For many applications of coherent optics where the wave front is measured or controlled (i.e., for the problems of object recognition, adaptive optics, etc.) it is important to investigate the peculiarities of the wave front behavior in the vicinity of dislocations of an optical field having speckle structure.

As a rule, the investigations are based on the analysis of complex polynomials, being formally the wave equation solutions. In this case the two-dimensional polynomials of not higher than the second order are commonly considered.<sup>1-3</sup> In this paper we consider three-dimensional polynomials. The results have been obtained on the basis of analysis of the integral solution of the parabolic wave equation (i.e., in the approximation of the Fresnel diffraction). In this approximation the wave field can be represented as

$$E(z, \rho) = \frac{k_0}{2\pi i z} \iint_{-\infty}^{\infty} d\rho_0 E_0(\rho_0) \times \exp\left\{ik_0z + \frac{ik_0(\rho - \rho_0)^2}{2z}\right\}, \tag{1}$$

where  $E_0$  is the initial wave field  $k_0$  is the wave number.

Let us assume that the initial field is formed by waves from  $N$  independent point sources

$$E_0(\rho_0) = \frac{2\pi i}{k_0} \sum_{k=1}^N A_k e^{i\alpha_k} \delta(\rho_k - \rho_0). \tag{2}$$

Then the field (1) is the result of the field interference from  $N$  point sources and takes the form:

$$E(z, \rho) = z^{-1} \sum_{k=1}^N A_k e^{i\varphi_k}, \tag{3}$$

where  $\varphi_k = k_0z + \alpha_k + k_0(\rho - \rho_k)^2/2z$ .

Assume that at the point  $\{z = z_0, \rho = 0\}$  the interference field vanishes, i.e.,

$$E(z_0, 0) = z_0^{-1} \sum_{k=1}^N A_k e^{i\varphi_{0k}} = 0, \tag{4}$$

where  $\varphi_{0k} = k_0z + \alpha_k + k_0\rho_k^2/2z_0$ .

The condition (4) is fulfilled when the following conditions are fulfilled simultaneously:

$$\begin{aligned} \sum_{k=1}^N A_k \cos \varphi_{0k} &= 0, \\ \sum_{k=1}^N A_k \sin \varphi_{0k} &= 0. \end{aligned} \tag{5}$$

Geometrically this can be represented as follows. One can see from Eq. (4) that the field at the dislocation point  $\{z_0, 0\}$  is the sum of complex numbers  $E_k = A_k e^{i\varphi_{0k}}$ . If every component corresponds to a vector on the plane, whose length is equal to  $A_k$ , and the angle between the vector and the axis  $OX$  is  $\varphi_{0k}$ , then the condition (4) indicates that the sum of vectors should be equal to zero. Hence, when representing the given sum of vectors geometrically on the plane, we obtain a closed broken line, i.e., the top of the last- $N$ th vector coincides with the origin of the first vector.

Thus, any  $N$ -angle polygon drawn on the plane, sets the relationship between  $A_k$  and  $\varphi_{0k}$ , according to which the field in the plane  $z = z_0$  has the dislocation at the origin of coordinates, i.e., at the point  $\rho = 0$ . This condition is used in numerical simulation of a speckle-field in the cases when it is necessary to know beforehand a true position of a dislocation.

From Eq. (3) we can determine the intensity and the Umov-Poynting vector of the speckle-field.

For the intensity we obtain

$$W(z, \rho) = E(z, \rho) E^*(z, \rho) = z^{-2} \sum_{k=1}^N W_k(z, \rho), \quad (6)$$

where  $W_k = \sum_{l=1}^N A_l A_k \cos[\varphi_l(z, \rho) - \varphi_k(z, \rho)]$ ;

$$\begin{aligned} \varphi_l(z, \rho) - \varphi_k(z, \rho) &= \\ &= \varphi_{0l} - \varphi_{0k} - \frac{k_0 \rho}{z} (\rho_l - \rho_k) + \frac{1}{2} \left( \frac{1}{z} - \frac{1}{z_0} \right) (\rho_l^2 - \rho_k^2). \end{aligned}$$

The transverse component of the Umov-Poynting vector is determined by the expression

$$\begin{aligned} \mathbf{P}_\perp(z, \rho) &= \frac{1}{k_0} \text{Im} \{ E^* \nabla_\rho E \} = \\ &= z^{-3} \sum_{k=1}^N (\rho - \rho_k) W_k(z, \rho). \end{aligned} \quad (7)$$

The behavior of the intensity and the Poynting vector in the vicinity of dislocations can be determined from Eqs. (6) and (7), when  $\rho$  in these expressions vanishes. Then the Taylor expansions of trigonometric functions are performed.

Thus we obtain

$$\begin{aligned} W &\cong a_x x^2 + a_y y^2 + 2 a_{xy} x y, \\ \mathbf{P}_\perp &\cong - \mathbf{e}_x a y + \mathbf{e}_y a x, \end{aligned} \quad (8)$$

where

$$\begin{aligned} \rho &= \{x, y\}; \quad \rho_k = \{x_k, y_k\}; \quad a = a_{cx} a_{sy} - a_{sx} a_{cy}; \\ a_x &= a_{cx}^2 + a_{sx}^2; \end{aligned}$$

$$\begin{aligned} a_y &= a_{cy}^2 + a_{sy}^2; \quad a_{xy} = a_{cx} a_{cy} + a_{sx} a_{sy}; \\ a_{cx} &= \sum_{k=1}^N A_k x_k \cos \varphi_{0k} = 0; \\ a_{sx} &= \sum_{k=1}^N A_k x_k \sin \varphi_{0k} = 0; \\ a_{cy} &= \sum_{k=1}^N A_k y_k \cos \varphi_{0k} = 0; \\ a_{sy} &= \sum_{k=1}^N A_k y_k \sin \varphi_{0k} = 0. \end{aligned} \quad (9)$$

From Eq. (8) it follows that at the point of dislocation and in its vicinity

$$|\mathbf{P}_\perp| \cong a |\rho|, \quad \text{rot } \mathbf{P}_\perp = 2 a.$$

We obtain the equation of degenerate curve of the second order when equating the expansion (8) for intensity to zero. In this case the invariant  $D$  of a given curve

$$D = \begin{vmatrix} a_x & a_{xy} \\ a_{xy} & a_y \end{vmatrix} = (a_{cx} a_{sy} - a_{sx} a_{cy})^2 = a^2$$

can be above zero or equals zero.

The condition  $D > 0$  corresponds to the case when the intensity reduces to zero at a separate point  $\rho = 0$ . The condition  $D = 0$  corresponds to the case of intensity vanishing on the line going through the point  $\rho = 0$ . For a given case  $\text{rot } \mathbf{P}_\perp = 0$ , since  $a = 0$ . The behavior of the Poynting vector and the phase in the vicinity of the point, where the intensity vanishes, has no peculiarities, typical for the spiral dislocation. Such a situation is observed, for example, at radiation diffraction on a circular or square hole when the intensity vanishes at closed lines or the lines becoming infinite.

The situation, typical for spiral dislocation, is presented in Fig. 1. The field of the Poynting vector in the plane is shown by arrows in Fig. 1 where we can clearly see two poles and a saddle point. The Poynting vector is connected with the intensity  $W$  and the phase  $\varphi$  of the resulting field by the following relation:

$$\mathbf{P}_\perp(z, \rho) = \frac{1}{k_0} W(z, \rho) \nabla_\rho \varphi(z, \rho). \quad (10)$$

The points of the poles are determined by the condition  $W = 0$ . In this case the phase is uncertain at the poles. The saddle point corresponds to the condition  $\nabla_\rho \varphi = 0$ . This picture is similar to that presented in Ref. 4, where the two-dimensional case was considered. However, in the three-dimensional case the behavior of energy streamlines, being considered, is strongly different.



FIG. 1. The Poynting vector field on the plane perpendicular to the propagation axis (arrows) and the projection of spatial energy streamline on a given plane (solid line).

Figure 1 shows this line projection on the plane perpendicular to the propagation axis. The origin of this line coincides with the plane, for which in the figure the Poynting vector field is represented. It is clear that the energy, having turned several times around the dislocation, escapes from it. Then the energy is captured by another dislocation and the process is repeated.

In this case, as the energy propagates, the dislocation itself shifts along the direction toward another dislocation (in this case, according to the linear law). As the dislocation comes closer, the energy, turned around dislocations, decreases and vanishes at the instant of their confluence. Then the dislocations, continuing on their way, diverge, having captured greater quantity of energy. Then they meet, on their way, other dislocations and the process is repeated.

For the two-dimensional case<sup>4</sup> the existence of limiting curves (limiting cycles) for the energy streamlines is typical. The limiting curves represent the boundaries opaque to energy, therefore the energy quantity, captured by the dislocation remains constant. This differences can be explained as follows. The equation for energy stream lines for the three-dimensional case is written as:

$$\frac{d\rho}{dz} = \frac{1}{k_0} \nabla_\rho \varphi(z, \rho) = \mathbf{P}_\perp(z, \rho) / W(z, \rho) \quad (11)$$

or

$$\begin{aligned} \frac{dx}{dz} &= P_x(z, x, y) / W(z, x, y), \\ \frac{dy}{dz} &= P_y(z, x, y) / W(z, x, y). \end{aligned} \quad (12)$$

For the two-dimensional case time plays the role of the coordinate  $z$  (evolution variable). In this case in Ref. 4 the situation is considered when in the right-hand side of Eq. (12) the dependence is lacking on the evolution variable and, hence, the paths are stationary. In our case we consider the optical wave propagation in a free space and stationary solutions are impossible.

Besides, the calculations of energy streamlines were performed based on the diffraction ray method,<sup>5</sup> which is based on the fact that the diffraction rays (energy streamlines) satisfy the equation<sup>6</sup>

$$\frac{d^2\rho}{dz^2} = \frac{1}{2} \nabla_\rho \varepsilon(z, \rho) + \frac{1}{2k_0^2} \nabla_\rho (A^{-1} \Delta_\rho A(z, \rho)), \quad (13)$$

where  $\varepsilon$  is the disturbance of dielectric constant,  $A$  is

the wave amplitude. In free space ( $\epsilon = 0$ ) this equation can be written in the form ( $W = A^2$ ):

$$\frac{d^2 \rho}{dz^2} = \frac{1}{4k_0^2} \nabla_{\rho} [W^{-1} \nabla_{\rho}^2 W - \frac{1}{2} W^{-2} (\nabla_{\rho} W)^2]. \quad (14)$$

The calculations, made by Eqs. (12) and (14), coincided within the errors of numerical calculations. This points, on the one hand to the applicability of the diffraction ray method in the given situation, and on the other hand, to the fact that the speckle-field intensity distribution contains the information on its vortex nature.

Let us consider the behavior of the speckle-field phase. As it was mentioned in Ref. 4, the phase sets the natural parametrization along the energy streamline since it is connected with the line length by a simple differential equation:

$$d\varphi = k_0 |\boldsymbol{\theta}| dl, \quad (15)$$

where  $\varphi$  is the phase,  $l$  is the line length,  $\boldsymbol{\theta}$  is the unit vector, whose direction coincides with the Poynting vector direction.

From Eq. (15) in the framework of paraxial approximation for the phase variation along the energy streamline the following expression is valid:

$$\varphi = k_0 \int_{z_0}^{z_1} dz [1 + \frac{1}{2} (\frac{d\rho}{dz})^2] = k_0 \int_{z_0}^{z_1} dz [1 + \frac{1}{2} (\mathbf{P}_{\perp} / W)^2]. \quad (16)$$

The phase difference between two arbitrary points lying in the same plane, perpendicular to the radiation propagation axis, can be calculated in the form:

$$\begin{aligned} \Delta\varphi_{\rho l} &= \int_{\rho_1}^{\rho_2} dl_{\perp} \nabla_{\rho} \varphi(z_0, \rho) = \\ &= k_0 \int_{\rho_1}^{\rho_2} W^{-1} [P_x dl_x + P_y dl_y], \end{aligned} \quad (17)$$

where  $d\mathbf{l}_{\perp} = \{dl_x, dl_y\}$  is the line element, connecting the points  $\rho_1$  and  $\rho_2$ ,  $\mathbf{P}_{\perp} = \{P_x, P_y\}$  is the transverse component of the Poynting vector. It should be noted that for a speckle-field this phase difference depends on the choice of the line connecting these points. For two different lines this difference is  $\pi$  by an even number, if the lines do not intersect the dislocations, and the above difference is  $\pi$  by an odd number, if one of the lines intersects one dislocation.

The following phase calculations have been made. In the plane  $z = z_0$  two points  $\rho_{01}$  and  $\rho_{02}$  were selected, whose phase difference calculated by the formula (17) along a straight line, connecting them,

equaled zero. The streamline paths were calculated, outgoing from a given points and intersecting the plane  $z = z_1$  at the points  $\rho_1$  and  $\rho_2$ , as well as the phase shifts along the given lines between the planes  $z = z_0$  and  $z = z_1$  by Eq. (16) ( $\varphi_1$  is the phase shift along the first line,  $\varphi_2$  - along the second line). The phase difference  $\Delta\varphi_{\rho l}$  between the points  $\rho_1$  and  $\rho_2$  in the plane  $z = z_1$  was calculated by formula (17) along a straight line (which did not intersect a dislocation). For any pair of lines the following relationship was obtained:

$$\varphi_1 - \varphi_2 = \Delta\varphi_{\rho l} + 2\pi n \quad (n \text{ is an integer number}). \quad (18)$$

As the initial point  $\rho_{01}$  approaches a dislocation, the number of rotations increases, which the energy streamline turns around the dislocation between fixed planes. With the increase in the number of such rotations the number  $n$  in Eq. (18) grows. And  $\rho_{01}$  tends to the dislocation point  $n$  approaches infinity.

Figure 2 shows the speckle-field phase distribution on the plane. There are 16 dislocations of wave field in the presented segment of the plane. The phase difference between the adjacent lines of the shading change is  $\pi/4$ . Eight shading degrees are given in the figure.

The following three figures (2b, 2c, and 2d) present the three interference pictures, every of which was obtained as a result of the speckle-field interference (3) with a plane wave

$$E_0(z, \rho) = A_0 e^{i k_0 z + i k_{\perp} \rho} = A_0 e^{i \varphi_0} \quad (19)$$

for the three different directions of the vector  $\mathbf{k}_{\perp}$ .

The interference of the fields (3) and (19) gives the following intensity distribution in the interference pattern:

$$W_I(z, \rho) = A_0^2 + 2 A_0 z^{-1} \sum_{k=1}^N A_0 \cos(\varphi_0 - \varphi_k) + W(z, \rho), \quad (20)$$

where  $W(z, \rho)$  is the speckle-field intensity (6). The lines of color exchange of the interference pattern correspond to the intensity level:

$$W_I(z, \rho) = A_0^2.$$

Thus it is seen that the interference patterns take the form of the «fractured[  
untwisted spiral. In this case the fracture points coincide with the speckle-field dislocation points. From Eq. (20) it follows that

$$\nabla_{\rho} W_I|_{\rho=0} = \frac{2 A_0}{z} \sum_{k=1}^N \rho_k A_k \sin\varphi_{0k}, \quad (21)$$

i.e., the value and the direction of the intensity gradient in the interference pattern at the dislocation point do not depend on the direction of the plane wave propagation (i.e., on the vector  $\mathbf{k}_{\perp}$ ) while the

interference pattern itself varies essentially when changing the plane wave direction. This fact is illustrated by Figs. 2 (*e* and *f*), where the corresponding fragments of the interference patterns, given in Figs. 2*c* and *d*, are magnified. The position of the speckle-field dislocation is denoted by the points. When performing the given numerical simulations of the speckle-field interference with a

plane wave, we have used the above-mentioned procedure for placing a dislocation at a given point of the plane. The segment of the straight line, coming from the dislocation point, corresponds to the direction and the value of the intensity gradient of interference pattern at a point of the speckle-field dislocation. The results of numerical simulation coincided with those by Eq. (21).

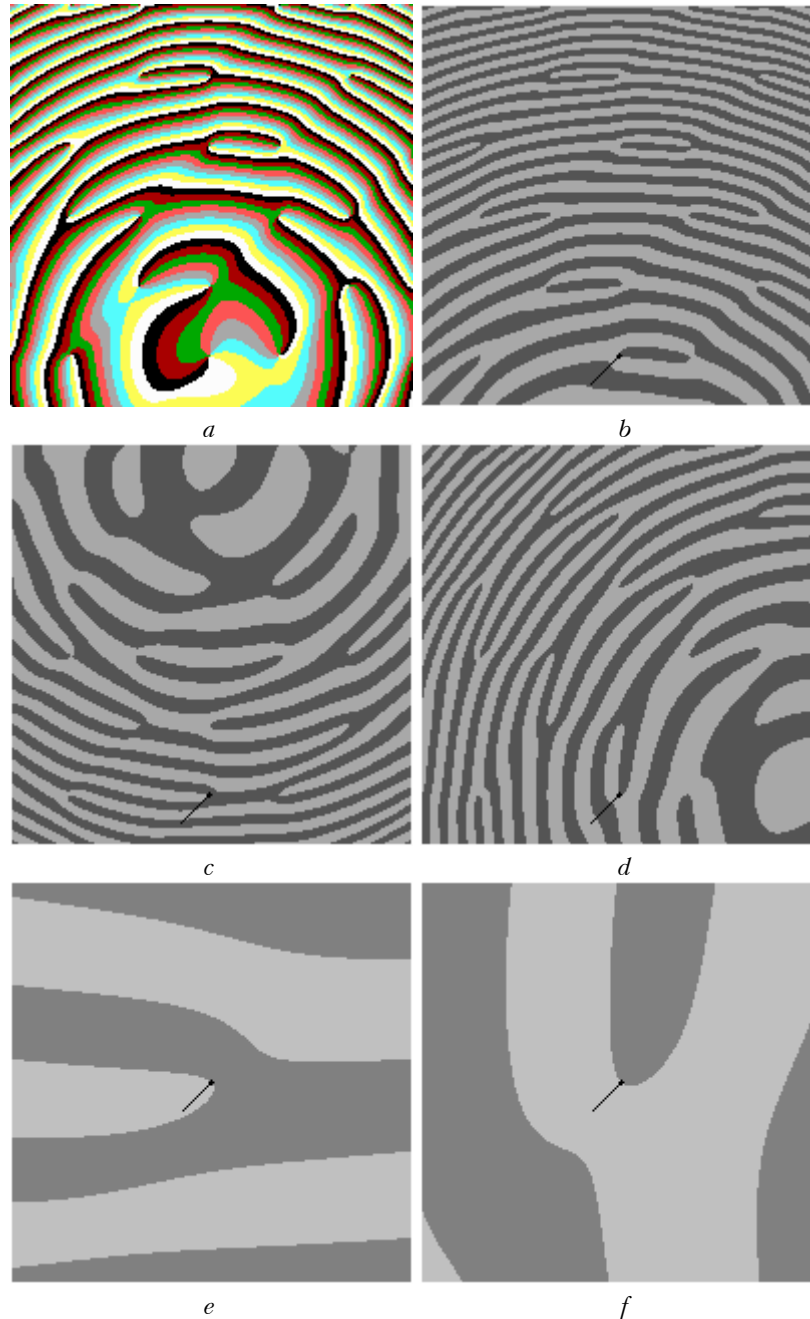


FIG. 2. The speckle-field phase distribution on the plane (*a*); the result of the speckle field interference with the plane waves of different directions (*b*, *c*, *d*); *e* and *f* are the magnified fragments of the interference patterns presented in Figs. 2 (*c*, *d*).

This fact enables one to determine, with a high accuracy, the position of dislocation of a given field on the plane using two (or more) interference patterns obtained from one speckle-field, since at superposition of the interference patterns the lines of color change of different interference patterns at dislocation points must touch one another.

In this paper we used the initial field representation in the form (2). From the viewpoint of derivation of theoretical results this approximation is quite acceptable. All the results obtained in this paper (for example, (5), (8), (9), (20), (21), etc.) can be written in the general case by substituting the summation over the finite number of the radiation plane points by integration over the whole plane. It is evident that such a substitution will not affect the conclusions, which have been drawn in the paper based on the above results.

At the same time, the representation (2) is necessary when making numerical simulations. Because even in the case when we simulate the radiation propagation from a continuous source we would have to pass from using continuous functions to the functions defined on a grid (given at the finite number of nodes) and from the integration over the surface to the summation over the finite number of nodes on a given surface.

It should be noted also that all the basic regularities of the speckle-field behavior, described in this paper, can be followed and an example is provided by the interference of waves from three point sources.

#### ACKNOWLEDGMENT

The work has been supported by the Russian Foundation for Fundamental Researches (Project 96-02-16382-a).

#### REFERENCES

1. J.F. Nye and M.V. Berry, Proc. Roy. Soc. London. **A336**, 165 (1974).
2. N.B. Baranova and B. Ja. Zel'dovich, Zh. Eksp. Teor. Fiz. **80**, 1789 (1981).
3. P.J. Wright and J.F. Nye, Phil. Trans. Roy. Soc. London **A305**, 339 (1982).
4. V.A. Zhuravleva, I.K. Kobozev, Yu.A. Kravtsov, Zh. Eksp. Teor. Fiz. **104**, 3769–3783 (1993).
5. V.V. Kolosov, Atmos. Oceanic Opt. **5**, No 4, 255–258 (1992).
6. V.I. Bespalov, A.G. Litvak, and V.I. Talanov, in: *Nonlinear Optics. Proceedings of the Second All-Union Symposium on Nonlinear Optics* (Nauka, Novosibirsk, 1968), 428–463.